Proceedings of the Second International Conference on Machine Learning and Cybernetics, Xi'an, 2-5 November 2003

OPTIMIZATION OF A CONDUCTANCE PROBE WITH VERTICAL MULTI-ELECTRODE ARRAY FOR THE MEASUREMENT OF OIL-WATER TWO-PHASE FLOW

NING-DE JIN, JUN WANG, LI-JUN XU

School of Electrical Engineering & Automation, Tianjin University, Tianjin 300072, China
E-MAIL: ndjin@mail.tju.edu.cn

Abstract:

This paper proposes a conductance probe with vertical multiple electrode array (VMEA) which can be used in oil-in-water two-phase pipe flow to measure the water volume fraction and axial velocity. The electrodes are flush mounted axially on the inside wall of an insulating duct. Using finite element analysis method, the evaluating indicators of uniform degree, spatial sensitivity and information volume were used to investigate the performance of the VMEA. The optimized VMEA has enhanced spatial sensitivity and capability of obtaining the distributed information from two-phase flow. Due to the significant difference of conductance between oil and water, the VMEA can also be used to measure gas-liquid and liquid-solid two-phase flow with conductive continuous phase. The evaluating indicators used in this paper can be used extensively to investigate other types of conductive probe.

Keywords:

Two-phase flow; Multi-electrode array; Analysis of sensitive filed; Probe optimization

1. Introduction

Oil-water two-phase flow is a common situation in oil logging and chemical engineering, so the measurement of oil-water is significant to the industrial process. A frequently used method of the measurement of two-phase flow is to set-up a theoretic model between volume fraction and the two-phase mixture impedance and apply cross-correlation algorithm to obtain the axial velocity of the mixture. The major advantages of this method are no interference to the flow, high frequency response, satisfying accuracy and the simplicity of industrial application. A comprehensive review of impedance method applied to two-phase flow was presented by Ceccio et al.[1].

With reference to the impedance method, a plate electrodes probe was employed by Coney [2] to investigate the theory behavior of flat electrodes for the measurement of liquid film thickness in two-phase flow. Dykesteen et al.[3] described a theoretic model used to relate the measured impedance and void fraction in three-component flow. Kytmöaa et al.[4] applied the guarded arc probe to validate the consistency of cross-correlation velocity and kinematic wave velocity. Tsochatzidis et al.[5] developed the mathematical model of Coney [2] to ring electrode system. Liu Xingbin [6] presented a four-ring-electrode conductive sensor for the measurement of water volume fraction. Chul-Hwa Song et al.[7] studied the void fraction using guarded arc probes and eliminated the error by introducing a reference probe. Fossa [8] investigated the performance of plate electrode and ring electrode. Devia&Fossa [9] designed the shape of probe along pipe circumference to obtain the linear dependence between the void fraction and the measured mixture conductance.

As far as axial velocity of two-phase flow is concerned, Lucas&Walton [10] applied a kinematic wave theory to measure the vertical upward bubbly two-phase flow. Lucas et al.[11, 12] embedded six ring electrodes on the surface of a mini insulating probe to measure liquid-solid two-phase flow and validate the ERT system. The ring conductance electrodes have been used by Lucas&Jin [13, 14] to measure oil-in-water two-phase flow using the modified kenematic wave theory. An axial six-electrode sensor was used by Hu Jinhai et al. [15] to obtain the water volume fraction and axial velocity of two-phase flow simultaneously.

Currently the plate electrode is applied to rectangular pipe and the arc or ring electrode is frequently used in cylinder pipes. The ring electrodes are mounted along the circumference of the pipe which has better spatial sensitivity. The performance of ring electrode array is decided by the electrode geometry, including the electrode height and the distance between the electrodes. Simultaneous measurement of volume fraction and velocity has been achieved using ring

0-7803-7865-2/03/$17.00 ©2003 IEEE

six-electrode array but the measurement of void fraction was attached to the cross-correlation velocity measurement electrodes. It is difficult to confirm its significance of optimization. The geometry of conductance probes used now is based on experience or simple analysis. An important aspect, the electric field edge effect of rings, is always not considered which could lead to unexpectable error. Therefore, there exist the problems of geometric optimization and electrode arrangement. There is still a lack of comprehensive study on the theoretic evaluating indicators, so it is necessary to improve the existing VMEA.

In order to tackle the problems discussed above, this paper proposes a probe with new geometry which can be employed to measure oil-in-water two-phase pipe flow. The optimum geometry figuration has been obtained by investigating the uniform degree, spatial sensitivity and information volume of the VMEA in a 125mm diameter cylinder pipe.

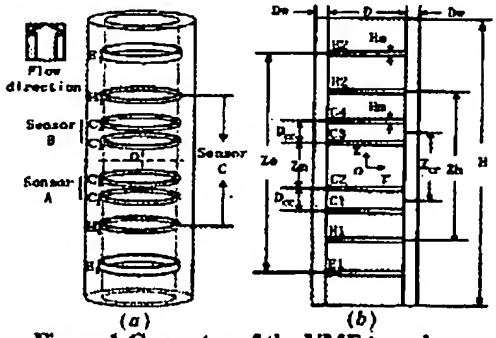

Figure 1 Geometry of the VMEA probe

2. Geometry of the VMEA for oil-in-water two-phase flow measurement

As shown by figure 1(a), the new VMEA consists of eight conductance rings which are flush mounted on the inside wall of the pipe. E_1 and E_2 are exciting electrodes. C_1-C_2 and C_3-C_4 are two up and down stream sensors denoted A and B respectively. H_1-H_2 are volume fraction sensor denoted C. All representing parameters used in this paper are shown in figure 1(b).

As electrodes E_1 and E_2 are excited by electrical source, the fluctuating signals across measuring electrodes (C_1-C_2, C_3-C_4 and H_1-H_2) reflect the conductance distribution of the two-phase flow. The signal from sensor C contains a mass of distributed information of oil-in-water two-phase flow, from which the water volume fraction can be obtained by a built model of water volume fraction. When two-phase mixture flows steadily inside the pipe, the signal from sensor A is similar to that from sensor B, on the basis of which the axial velocity can be obtained using cross-correlation algorithm. In this study, oil-in-water dispersed bubbly flow is assumed to find the optimum configuration of the VMEA.

3. Optimization of exciting electrodes

3.1 The analysis of sensitive field of the VMEA

The measuring principle of the VMEA is due to the theory of sensitive field. In order to prevent the corrosion of those electrodes and the electrolysis of two-phase mixture in the vicinity of electrodes, the titanium alloy material and alternating voltage are applied. It is usually decided to keep the exciting

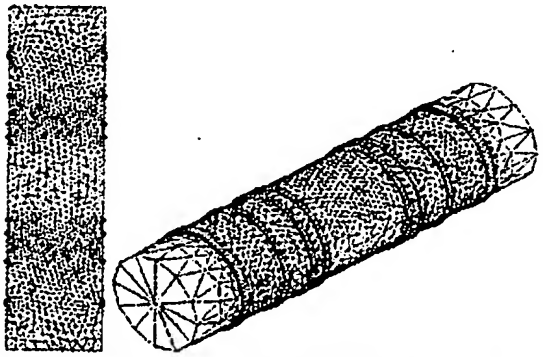

Figure 2 The meshed 2D and 3D finite element model

frequency of the applied voltage in the range of less than 100 KHz to eliminate the role of capacitance. For the inner pipe diameter is much small in comparison to the wavelength of the sensitive field, the electric field can be modeled as time-invariant, so Laplace equation $\nabla^2 U = 0$ of static field can be used.

The 2D and 3D models are meshed with triangle and tetrahedron respectively, which are shown as figure 2. Material properties of electrodes and fluid mixture are taken into account. The both ends of pipe should be assumed as infinite reference plane to eliminate the calculation error. One point worth noticing from the FE meshing is that the mesh cells should be fine enough to figure out the interfacial effect between electrodes and fluids.

The simulation is performed for all electrodes thickness of 1mm, exciting electrodes E1 and E2 positioned at $z = \pm Ze/2$ and ±10V voltage supplied. The electric field distribution is shown as figure 3. As can be

seen, in the region adjacent to E_1 and E_2, the distribution of voltage U is very peaky and approximately equal to the applied voltage, while in the range far from E_1 and E_2, the U is tend to be linear. Figures 3(a) and 3(b) show that in the vicinity of E_1 and E_2, both of the current density J_r and J_z vary sharply. Within the scope between exciting electrodes, the J_r and J_z distribute uniformly and tend to be constant. Here this region is defined as uniform field region. Previous works have presented measuring electrodes should be set in this region, but further investigation in this study show that the optimum probe configurations are far beyond the previous works.

3.2 The effect of H_e on sensitive field

For uniformly dispersed bubbly oil-in-water flow, the sensitive field distribution is mainly effected by the height and distance of exciting electrode.

The axial length of the uniform field section will be used following, of which quantization error is confined in the range less than 1%. The current density near the pipe wall and axis is denoted J_W and J_A respectively. In order to investigate the uniform degree (UD) of the sensitive field along the radial and axial direction, the radial UD and axial UD are defined and denoted X_{UD} and Y_{UD}. X_{UD} and Y_{UD} can be calculated using the equations below:

$$X_{UD}=\frac{(|J_w|-|J_A|)}{(|J_w|+|J_A|)/2}\times 100 \quad Y_{UD}=\frac{L_{UF}}{Z_e}\times 100 \quad (1)$$

where L_{UF} is the length of the uniform field region. The curves of J and X_{UD} are shown as figure 4 (Very little variation of Y_{UD} is observed, so the Y_{UD} is not shown here). It can be seen that J increases with H_e but X_{UD} decreases. As known, the polarization will increases with the expansion of interface between electrode and mixture, therefore 5mm is best.

3.3 The effect of Z_e on sensitive field

Several evaluating indicators of sensitive field are calculated and shown as figure 5. As can be seen, the uniformity of field distribution can be improved with the increase of Z_e, but the current density J declines simultaneously. It is difficult to determine the value of Z_e, so further works are performed following.

Since the edge effect of electric field, some part of the potential distribution is outside of the region between electrode E_1 and electrode E_2. As a result, the output of the VMEA will unavoidably include the ineffective distributed information of the fluid body. So the further work must be carried out to minimize the ineffective information.

4. Optimization of volume fraction electrodes

4.1 Spatial sensitivity distribution of volume fraction electrodes

The water volume fraction can be obtained by the equivalent mixture conductance which contains the fluid information. The capability of getting information from fluid region is decided by the spatial sensitivity of measuring electrode, so the investigation of spatial sensitivity and the capability of obtaining information is necessary.

Lucas *et al.*[11,12] investigated the spatial sensitivity of the axial six-electrode local probe which was inserted into the pipeline. The Lucas spatial sensitivity is used here. It is assumed that a small non-conducting fluid particle is positioned in the pipe with its center at coordinates (r,z) in r-z plane. $\delta U(r,z)$ is the change in voltage drop on the measuring electrode pair. Then the sensitivity of the measuring sensor $\Psi(r, z)$ is defined as:

$$\psi(r,z)=\frac{\delta U(r,z)}{(\delta U)_{max}}\times 100 \quad (2)$$

where $(\delta U)_{max}$ is the maximum $\delta U(r,z)$, then the sensitivity of sensor C can be calculated and denoted $\Psi_C(r,z)$. The calculated distribution of $\Psi_C(r,z)$ is shown in figure 10. It can be seen that the $\Psi_C(r,z)$ is high relative to that round the pipe axis in the region close to electrodes H_1 and H_2. The plot shows four distinct peaks alongside of the pipe wall. Clearly the spatial sensitivity is symmetrically distributed. One of the outboard peaks is between the electrodes H_1 and E_1 whilst the other is between electrodes H_2 and E_2. Both inboard peaks are between electrodes H_1 and H_2 and close to the corresponding electrode.

In order to explicitly analyze the effect of the probe configuration on the spatial sensitivity distribution, here define the sensitivity along r axial as eigen sensitivity function denoted $\psi_C(r,z)|_{z=0}$ and calculated for a wide range of electrode geometries. As figure 6 shown, $\psi_C(r,0)$ is determined by Z_e and Z_h. The plot exhibits significant difference between $\psi_C(r,0)$ close to the pipe wall and round the pipe axis as Z_e is equal to 100mm. The approximately horizontal curve appears when Z_e=200mm and Z_e=300mm, which means the electrode pair C can obtain approximately equal information from various fluid region.

4.2 Information of volume fraction electrodes

The capability of obtaining fluid information should be enhanced when the spatial sensitivity distributed uniformly. Primarily, the fluid distributed information should be quantitated. The information volume is defined as:

$$V_f(r,z) = \int_s \psi ds = \iint_s \psi(r,z)drdz \qquad (3)$$

where V_f is the obtained total information volume of measuring electrode and where S is the region of measuring electrode pair. It can be seen from figure 10 that $\Psi_C(r,z)$ covers some part of the region outside the sensor C, with the result that some ineffective information is included unexpectively. The investigation of effective information should be performed. Effective information can be expressed as:

$$V_{EI}(r,z) = 2\int_0^R \int_{-Z_s/2}^{Z_s/2} \psi(r,z)drdz \qquad (4)$$

where V_{EI} is the effective information volume and the integral region is the field between the measuring electrodes. The concentration of V_{EI} in V_f is calculated using the expressions as below:

$$C_{EI}(r,z) = \frac{V_{EI}(r,z)}{V_f(r,z)} \times 100 \qquad (5)$$

The information volume curves of sensor C are shown as figure 7, where V_{f_C}, V_{EI_C} and C_{EI_C} denote the total information volume, effective information volume and concentration of effective information respectively. It can be seen that V_{f_C} and V_{EI_C} has always a maximum value and C_{EI_C} increases when they are calculated for a wide range of electrode geometries. For measuring electrodes, the criterion to determine the value of Z_h should be that it can get as most effective information as possible from the measured fluid region.

It is worthwhile to notice that there is little interaction between volume fraction sensor C and cross correlation sensors A and B, so the investigation of sensors A and B can be performed without modeling volume fraction sensor.

5. Optimization of cross-correlation electrodes

Lucas *et al.*[12] described that the 'sensing volume' should be compact enough to keep high accuracy of the transition spacing of the fluid body flowing from upstream sensor A to downstream sensor B which is denoted Z_{CC}(see figure 1(b)). In order to get accurate transit time, the C_{EI} of sensor A and sensor B should be the maximum value.

According to the spatial sensitivity defined in equation (2), the spatial sensitivity of sensor A and sensor B are denoted $\Psi_A(r,z)$ and $\Psi_B(r,z)$ respectively and calculated in a similar way to $\Psi_C(r,z)$. Figure11 exhibits the symmetrical relation between $\Psi_A(r,z)$ and $\Psi_B(r,z)$. The peak of $\Psi_A(r,z)$ is approximately midway between electrodes C_1 and C_2 whilst the peak of $\Psi_B(r,z)$ is approximately midway between electrodes C_3 and C_4. The peak value is defined as the eigenvalue to investigate its variational regulation. The calculated eigenvalue distribution is shown as figure 8, of which the influencing factors are Z_{CC}, Z_e and D_{CC}. It can be seen that as the position of sensors A and B is towards the center region of the VMEA, $\Psi_A(r,z)$ and $\Psi_B(r,z)$ decreases simultaneously, hence sensors A and B should be not too close. Since the position of Ψ_A=100(or Ψ_B=100) always appears as D_{CC} is equal to 20mm, an important conclusion can be drawn apparently from figure 8 is that the optimum value of D_{CC} should be 20mm.

As figure 11 shown, some part of $\Psi_A(r,z)$ is outside of the effective region of sensor A whilst some part of $\Psi_B(r,z)$ is outside of the effective region of sensor B, which demonstrates that ineffective information exists in the total information of the output cross sensors A and B. In order to get accurate transit time, the concentration of effective information of sensor A and sensor B is investigated for D_{CC}=20mm(Figure 9). As the position of sensor A (or B) is towards electrode E_1 (or E_2) and far from the position z=0, C_{EI_A} and C_{EI_B} decrease, where C_{EI_A} and C_{EI_B} are the concentration of the effective information of cross-correlation electrodes A and B. As Z_e increases, C_{EI_A} and C_{EI_B} decrease as well. All the evaluating indicators should be taken into account as the optimum probe configuration is to be determined.

As demonstrated by figure 7, there always exists a maximum of V_{EI_C} for each group of Z_h and Z_e and the difference between the every two maximums is distinct. Figure 6 shows the approximately horizontal $\Psi_C(r,0)$ curve appears when Z_e is over 200mm. The distinct difference between the sensitivity of sensor A and sensor B can also be seen in figure8. Taking above discussions into account, 250mm should be the best value of Z_e, then Z_h=170mm can be obtained from figure 7. Figure 10 also shows 55mm is the preferable C_{EI_A} or C_{EI_B}, the corresponding Z_{CC} is 110mm. The spatial sensitivity distribution of the optimized VMEA is shown in figure 10 and figure 11.

6. Conclusions

Based on Laplace problem of electric field of the VMEA and the systematic evaluating indicators, the geometry of vertical multiple electrode conductive array is optimized. The characteristics of the optimized VMEA can be concluded as below:

The volume fraction sensor is separated from cross-correlation sensors, which can enhance the spatial sensitivity and capability of acquiring equal information from fluid regions.

The cross-correlation sensors have maximum concentration of effective information and small measuring space, which guarantee that accurate measurement of fluid velocity can be achieved.

The optimized VMEA can measure volume fraction and the fluid velocity of oil-in-water two-phase flow simultaneously.

References

[1]. S.L. Ceccio and D.L. George, A review of electrical impedance techniques for the measurement of multiphase flows. Journal of Fluids Engineering-Transactions of the ASME. Vol.118, No.2, pp. 391-399, 1996

[2]. M.W.E. Coney, The theory and application of conductance probes for the measurement of liquid film thickness in two –phase flow, J. Phys. E: Scient. Instrum., Vol. 6, pp. 903-910, 1973

[3]. Eivind Dykesteen, Anders Hallanger, Erling Hammer, Edmund Samnoy and Richard Thorn., Non-intrusive three-component ratio measurement using and impedance sensor, J. Phys. E: Sci. Instrum., Vol.18, 1985

[4]. H.K. Kytömaa and C.E. Brennen, Small amplitude kinematic wave propagation in two-component media, Int. J. Multiphase Flow Vol.17, No.1, pp. 13-26, 1991

[5]. N.A. Tsochatzidis, T.D. Karapantsios, M.V. Kostoglou and A.J. Karabelas, A conductance probe for measuring liquid fraction in pipes and packed beds, Int. J. Multiphase Flow Vol. 18, No. 5, pp. 653-667,1992

[6]. Liu Xingbin, Downhole measurement of oil/water two-phase flows, Ph. D. Dissertation, 1996

[7]. Chul-Hwa Song, Moon Ki Chung, Hee Cheon No, Measurements of void fraction by an improved multi-channel conductance void meter, Nuclear Engineering an Design ,Vol. 184, pp. 269-285, 1998

[8]. M. Fossa, Design and performance of a conductance probe for measuring the liquid fraction in two-phase gas-liquid flows, Flow Meas. Instrum., Vol. 9, pp. 103-109,1998

[9]. F. Devia and M. Fossa, Geometry optimization of impedance probes for void fraction measurements, ICMF, 2001

[10]. G.P. Lucas and I.C. Walton, Flow rate measurement by kinematic wave detection in vertically upward bubbly two-phase flows, Flow Meas. Instrum. Vol. 8. pp. 133-143, 1997

[11]. G.P. Lucas, J. Cory, R.C. Waterfall, W.W. Loh and F.J. Dickin, Measurement of the solids volume fraction and velocity distributions in solids-liquid flows using dual-plane electrical resistance tomography, Flow Meas. Instrum., Vol. 10. pp. 249-258, 1999

[12]. G.P. Lucas, J.C. Cory and R.C. Waterfall, A six-electrode local probe for measuring solids velocity and volume fraction profiles in solids-water flows, Meas. Sci. Technol, Vol. 11, pp. 1498-1509 , 2000

[13]. G.P. Lucas and N.D. Jin, Measurement of the homogeneous velocity of inclined oil-in-water flows using a resistance cross correlation flow meter, Meas. Sci. Technol. Vol.12, pp. 1529-1537, 2001

[14]. G.P. Lucas and N.D. Jin, A new kinematic wave model for interpreting cross correlation velocity measurements in vertically upward bubbly oil-in-water flows, Meas. Sci. Technol., Vol.12, pp.1538-1545, 2001

[15]. Hu Jinhai, Liu Xingbin Huang Chunhui, Zhang Yuhui, Qiao Zhuoer, A conductance sensor for simultaneously measuring flowrate and watercut in oil/water two-phase flow, Well Logging Technology(in Chinese), Vol. 26(2), pp. 154-157, 2002

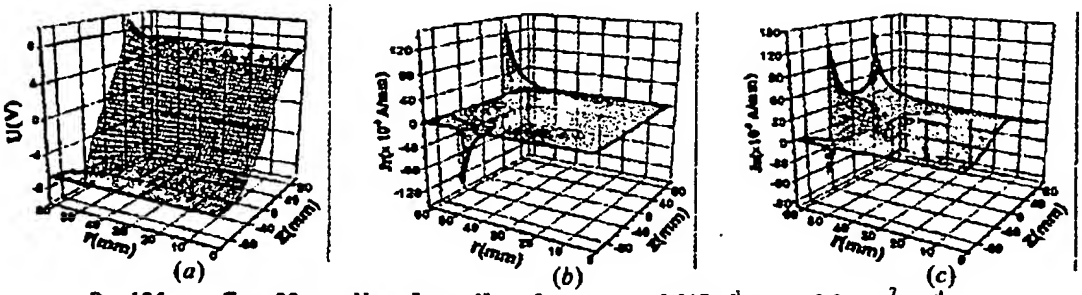

$D = 125$mm, $Z_e = 90$mm, $H_e = 5$mm, $H_m = 3$mm, $\sigma_w = 0.01\mathrm{Sm}^{-1}$, $\sigma_{Ti} = 2.3\times10^{7}\,\mathrm{Sm}^{-1}$, $\alpha = 1$

σ_w – water conductivity, σ_{Ti} – conductivity of titanium, α – water volume fraction

U – voltage distributed in the VMEA, Jr – the component of current density in radial direction

Jz – the component of current density in axial direction

Figure 3 Spatial sensitivity distribution of the volume fraction sensor C

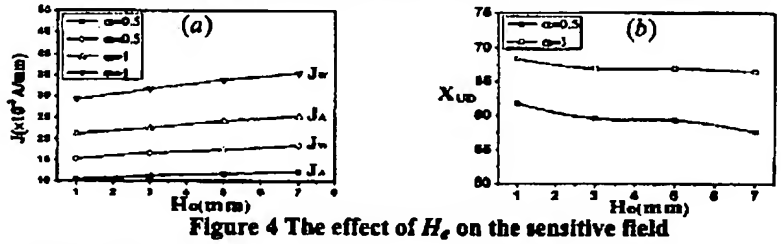

Figure 4 The effect of H_e on the sensitive field

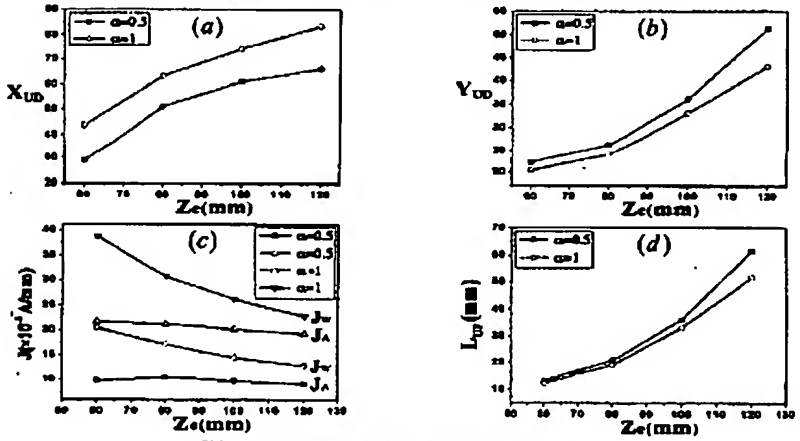

Figure 5 The effect of Z_e on the sensitive

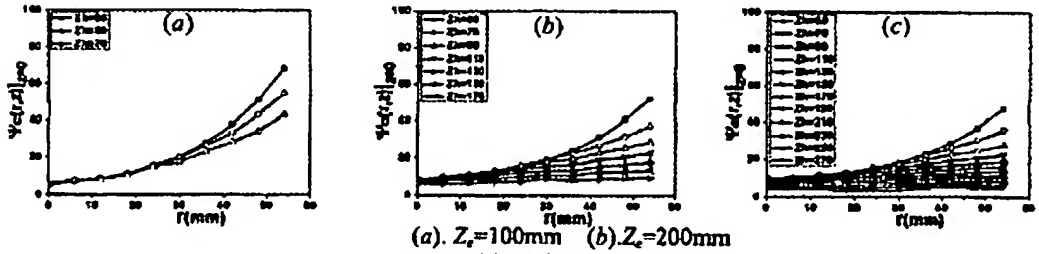

(a). Z_e=100mm (b).Z_e=200mm

(c).Z_e=300mm

Figure 6 Eigen sensitivity distribution of sensor C

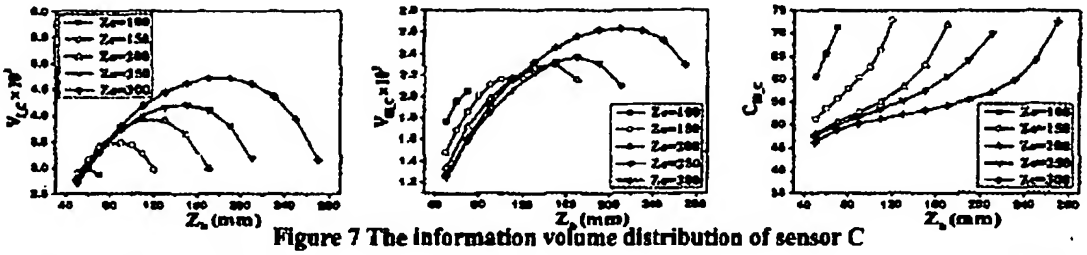

Figure 7 The information volume distribution of sensor C

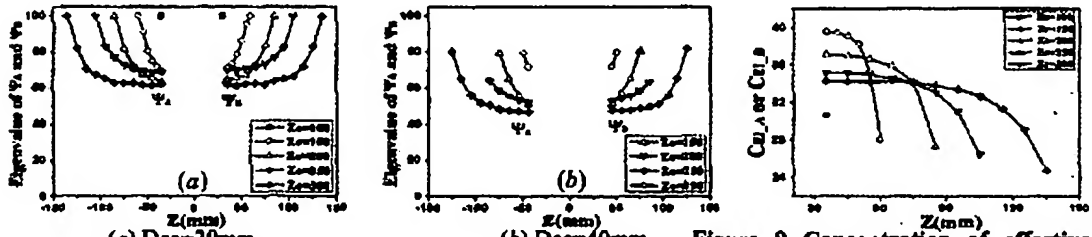

(a) Dcc=20mm (b) Dcc=40mm

Figure 8 Eigenvalue distributions of cross-correlation sensors

Figure 9 Concentration of effective information of sensor A or sensor B

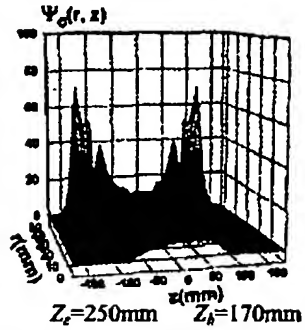

Z_e=250mm Z_h=170mm

Figure 10 Sensitivity distribution of sensor C

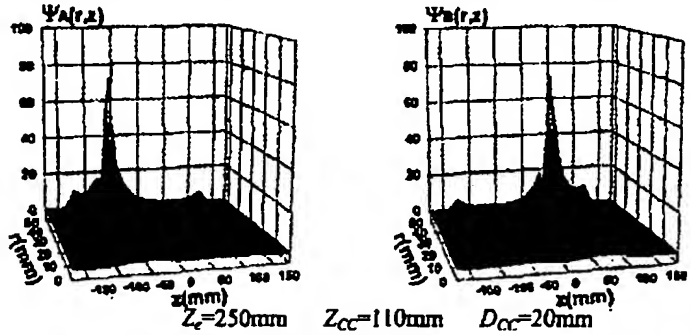

Z_e=250mm Z_{CC}=110mm D_{CC}=20mm

Figure 11 Sensitivity distribution of sensor A and sensor B